

PAPER • OPEN ACCESS

Suppression of backward scattering using chain of high index dielectric nanospheres

To cite this article: Misael Natanael and Alexander A Iskandar 2020 *J. Phys.: Conf. Ser.* **1552** 012006

View the [article online](#) for updates and enhancements.

You may also like

- [Dielectric optical nanoantennas](#)
Md Rabiul Hasan and Olav Gaute Hjeltnes
- [Symmetric relationship of multiple scattering in birefringent slab media: Monte Carlo simulation](#)
Soichi Otsuki
- [Resonant dielectric nanostructures: a low-loss platform for functional nanophotonics](#)
Manuel Decker and Isabelle Staude



PRIME
PACIFIC RIM MEETING
ON ELECTROCHEMICAL
AND SOLID STATE SCIENCE

HONOLULU, HI
Oct 6–11, 2024

Abstract submission deadline:
April 12, 2024

Learn more and submit!



Joint Meeting of

The Electrochemical Society
•
The Electrochemical Society of Japan
•
Korea Electrochemical Society

Suppression of backward scattering using chain of high index dielectric nanospheres

Misael Natanael and Alexander A Iskandar*

Physics of Magnetism and Photonics Research Division, Institut Teknologi Bandung,
Jl. Ganesa 10, Bandung 40132, Indonesia

*Corresponding author: iskandar@fi.itb.ac.id

Abstract. High refractive index dielectric materials have been widely studied in nanophotonics as a substitute for plasmonic materials due to its low dissipative losses and its ability to generate magnetic moments resonance in visible light spectrum. The dimension, geometry, and materials used will affect the excited multipole moments, this can in turn be used to tailor the scattered field. The aim of this study is to design a structure composed of silicon nanospheres arranged in chain-like configuration which can suppress backward scattering. Analytical Mie theory formulation is employed to calculate the scattering field. Results show that by increasing the gap distance between nanospheres at certain incident wavelength, forward-to-backward scattering ratio is increased until it reaches optimum value. Further increase will enhance backward scattering due to higher multipole excitation.

1. Introduction

In nanophotonics, nanoparticles are widely used to construct devices which can control light in nanometer scale. Early investigation employed plasmonic materials (noble metals surrounded by dielectric environment) to manipulate light. However, plasmonic materials suffer from high dissipative losses due to generation of conduction current. As an alternative, high refractive index dielectric materials have been widely used because of its low dissipative losses and furthermore additional degrees of freedom are obtained from its ability to generate magnetic resonance in visible region [1]. High-index dielectric nanoparticles have been used for designing nanoantennas [2], steering light beam [3], and suppressing backward scattering [4]. Those control of light can be achieved by tailoring the excited multipole moments generated within the nanostructure. Among these light control via dielectric particles, suppression of backward scattering have been a common research in nanophotonics. Several studies showed that this phenomena can be optimized by selecting proper materials with fixed spherical geometry [5] or by using spheroidal particle with certain optimum shape parameters [4]. Another approach that can possibly optimize this phenomena is by using multiple nanospheres with fixed geometry and search for its spatial configuration (positions of each spheres for example) which yield optimum suppression of backward scattering. This scheme would be relatively simple because we only have to change the positions of each nanospheres. In this study, a colinearly arranged nanospheres structure is considered. By designing the spatial configuration, we can control the scattering ratio between forward and backward scattering which can leads to suppression of backward scattering. This ability to control the forward and backward scatterings could be useful the design of optical device and become the building block of metamaterials.



2. Analytical Mie Theory

For this study, the analytical and rigorous Mie scattering theory for spherical particles was employed to analyze the scattering field characteristics of the structure. In this theory, the fields are expanded into vector spherical harmonics (VSH). In particular, the expansion of the incident and scattered fields can be written as [6]

$$\mathbf{E}_i = -\sum_{n=1}^{\infty} \sum_{m=-n}^n iE_{mn} \left(p_{mn} \mathbf{N}_{mn}^{(1)} + q_{mn} \mathbf{M}_{mn}^{(1)} \right) \quad (1)$$

$$\mathbf{E}_s = \sum_{n=1}^{\infty} \sum_{m=-n}^n iE_{mn} \left(a_{mn} \mathbf{N}_{mn}^{(3)} + b_{mn} \mathbf{M}_{mn}^{(3)} \right) \quad (2)$$

where $E_{mn} = E_0 i^n (2n+1) \frac{(n-m)!}{(n+m)!}$ and E_0 is the amplitude of incident field. The coefficients p_{mn} and q_{mn} are the expansion coefficients for incident field which depends only on the characteristics of the incident wave, while a_{mn} and b_{mn} are the expansion coefficients for scattered field that must be determined. Here $\mathbf{M}_{mn}^{(j)}$ and $\mathbf{N}_{mn}^{(j)}$ are the VSH which act as the basis function for field expansion. Superscript j indicates the spherical Bessel function used in the VSH form ($j=1$ refers to spherical Bessel function of the first kind, $j=3$ refers to spherical Hankel function of the first kind).

The scattering coefficients can be obtained by solving system of linear equations

$$a_{mn}^j = a_n^j \left(p_{mn}^{j,j} - \sum_{l \neq j}^L \sum_{v=1}^{\infty} \sum_{\mu=-v}^v \left[a_{\mu\nu}^l A_{mn}^{\mu\nu} + b_{\mu\nu}^l B_{mn}^{\mu\nu} \right] \right) \quad (3)$$

$$b_{mn}^j = b_n^j \left(q_{mn}^{j,j} - \sum_{l \neq j}^L \sum_{v=1}^{\infty} \sum_{\mu=-v}^v \left[a_{\mu\nu}^l B_{mn}^{\mu\nu} + b_{\mu\nu}^l A_{mn}^{\mu\nu} \right] \right) \quad (4)$$

Here, a_n^j and b_n^j are Mie coefficients for single isolated sphere [7], L is the number of particles to be considered, and $A_{mn}^{\mu\nu}$ and $B_{mn}^{\mu\nu}$ are translation coefficients which depend on relative position between the particles. The latter have to be used in order to transform the fields between particle's coordinate system. Once the scattering coefficients have been obtained, fields, intensity, and cross section could then be calculated. The contribution from certain multipole term can be obtained by taking the corresponding Mie mode term [8]. The coefficient a are related to electric Mie multipole modes and the coefficient b are related to the magnetic Mie multipole modes, while the second subscript determine the type of the Mie modes. For example, in equation (2), a_{mn} terms for $n=1$ corresponds to electric dipole contribution, b_{mn} terms for $n=2$ corresponds to magnetic quadrupole contribution, etc.

3. Results and Discussion

Here we consider a structure consisting of three silicon (Si) nanospheres with radius R_1 , R_2 , and R_3 respectively. This structure is arranged in colinear (chain-like) configuration and embedded in background medium with refractive index $n_b = 1$. The surface-to-surface distances between each spheres are denoted by D and d . This structure is illuminated by x -polarized electromagnetic plane wave propagating in z direction (**Figure 1**). Silicon is chosen as the materials for nanospheres because it exhibits high refractive index and little absorption losses [9].

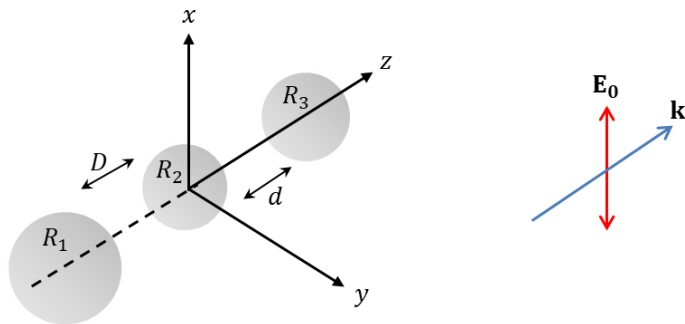


Figure 1. System being considered which consists of three Si nanospheres each of radius R_1 , R_2 , and R_3 , gap distances D and d between the spheres.

We consider the configuration in which D is varied while the other parameters are kept constant. The radius of each nanospheres are $R_1 = 110$ nm, $R_2 = R_3 = 70$ nm and the gap distance between the second and the third nanosphere is $d = 8$ nm. We calculate the forward-backward scattering intensity ratio (I_{fwd} / I_{bck}) at far field zone $r \approx 2$ μ m. For silicon refractive index data, Ref. [10] is used.

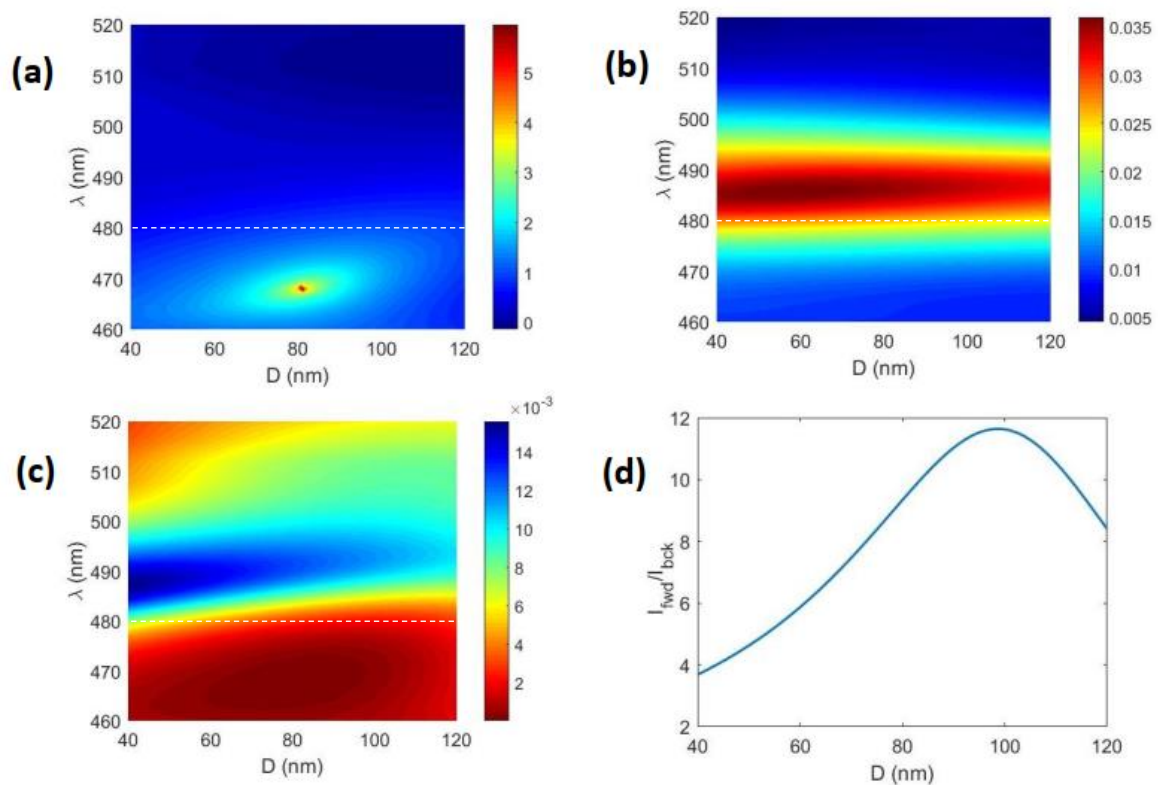


Figure 2. Colormaps which represent (a) logarithmic value of I_{fwd} / I_{bck} , (b) forward intensity I_{fwd} , (c) backward intensity I_{bck} (with flipped colorbar scale) as functions of gap distance D and incident wavelength λ . (d) Cross section of I_{fwd} / I_{bck} colormap at $\lambda = 480$ nm.

Figure 2(a) shows the logarithmic value of forward-backward ratio as functions of gap distance D and incident wavelength λ (visualized as colormap). Forward and backward scattering intensity are shown on **Figure 2(b)** and **Figure 2(c)** respectively. For I_{bck} colormap, the colorbar scale is flipped

(red corresponds to small intensity while blue corresponds to high intensity) in order to show that we expect small backward intensity. From **Figure 2(a)**, we can see that the forward-backward scattering ratio reaches maximum value at $D = 81$ nm and $\lambda = 468$ nm. The order of magnitude of this maximum value is 5 ($I_{fwd} / I_{bck} \approx 10^5$), the backward scattering is nearly zero, however, the forward scattering intensity is quite small compared to another configuration as can be seen from **Figure 2(b)**. For comparison, **Figure 3** shows the radiation polar plot in 3 different cases. The orange solid line refers to the case where backward scattering almost zero yielding a forward-backward ratio of 467.54, but the forward scattering is quite small. The red dashed line refers to the case where forward-backward scattering ratio is in the order of magnitude of 1. Although the ratio is small, the forward scattering is quite high and backward scattering is appreciably small. The blue dashed-dot line has the highest value of forward-backward intensity difference ($I_{fwd} - I_{bck}$) whereas its ratio is of the value 5.46. From this analysis, it can be seen that the forward-backward scattering ratio cannot always be used as a guideline for designing nanospheres system. Careful investigation of each forward and backward intensity must be employed in order to avoid misinterpretation from the simulation results.

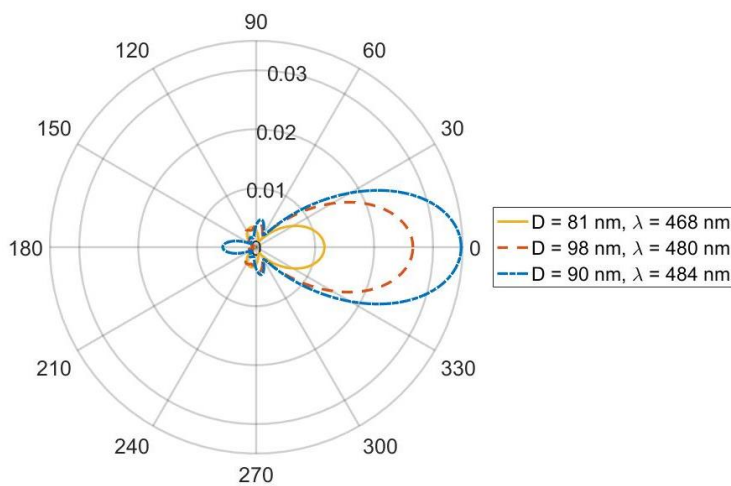


Figure 3. Radiation polar plot at far field zone in xz plane. The angle 0° corresponds to forward direction while 180° corresponds to backward direction. Each color line refers to different values of D and λ with different characteristics of forward and backward scattering.

For further analysis, take a cursory example of the cross section in **Figure 2(a)** at $\lambda = 480$ nm as shown in **Figure 2(d)**. As the gap distance increased, the forward-backward scattering ratio also increased (which means that the backward scattering suppressed) until it reaches some maximum value. If the distance is increased further, the ratio will be decreased. This result means that there is an optimum value of D which has the largest forward-backward ratio. This feature can be explained by analyzing the multipole contribution for scattered field.

Figure 4 shows the real part of the scattered electric field at x -component for each Mie multipole modes as a function of D . The field from electric quadrupole (EQ) and magnetic octupole (MO) has opposite sign compared to the electric hexadecapole (EHD). As D increased, EQ and MO fields tends to enhance the forward and suppress the backward resultant fields, while the EHD field has opposite role (which enhance the backward and suppress the forward fields). At certain value of D , this competing EHD field win against those two former fields. From this analysis, we can see that the larger distance between nanospheres could generate higher multipole modes. Radiation plot at three different values of D are shown in **Figure 5**. We can see that the tail of backward radiation pattern has its smallest value at $D = 98$ nm which corresponds to largest forward-backward scattering ratio of 11.58.

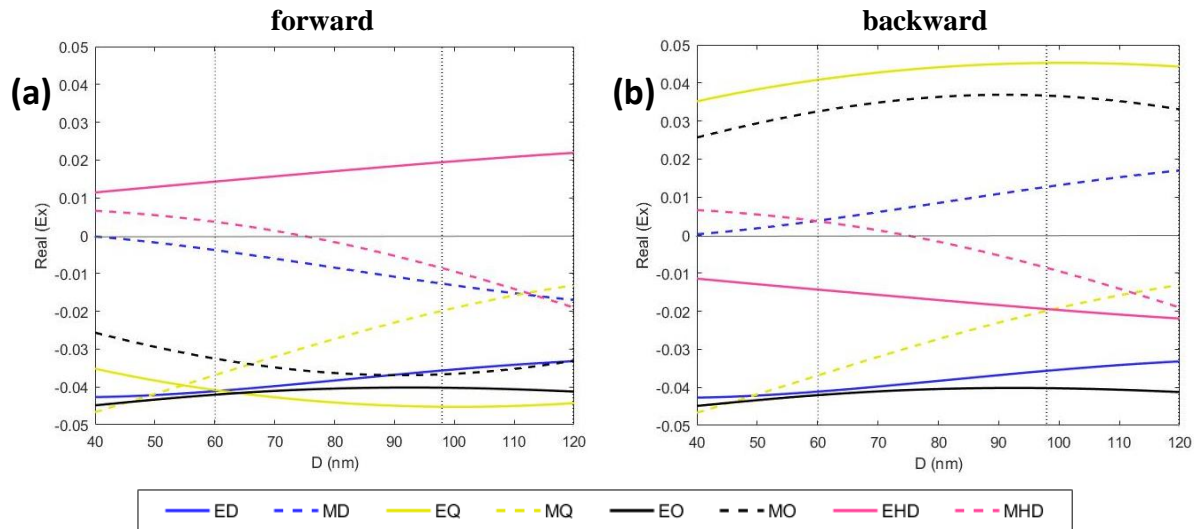


Figure 4. The real part of the scattered electric field at x direction as a function of gap distance D for each multipole modes (dipole, quadrupole, octupole, and hexadecapole) at $\lambda = 480$ nm. These fields are calculated at forward (a) and backward (b) direction respectively.

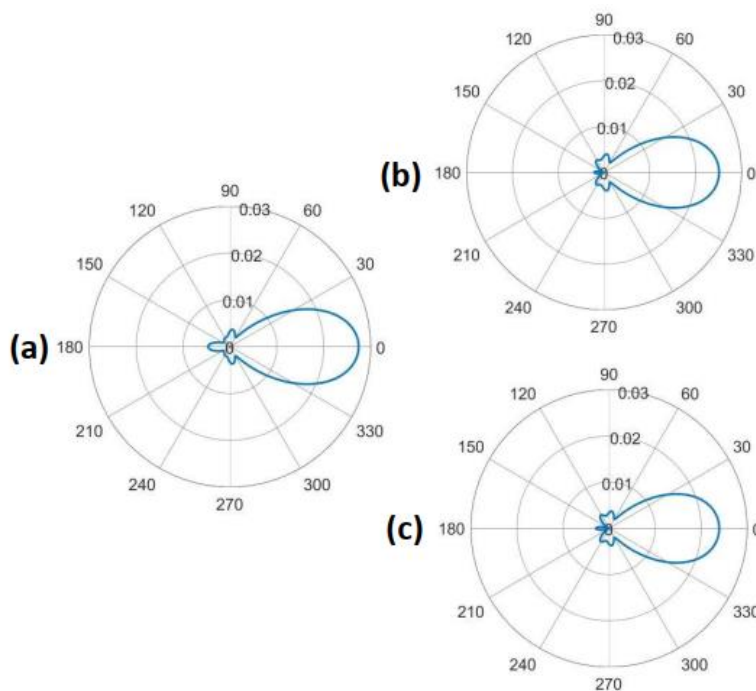


Figure 5. Radiation polar plot (in xz plane) for different values of D at $\lambda = 480$ nm : (a) 60 nm, (b) 98 nm, and (c) 120 nm.

It is well known that a system of single nanosphere can also be used to suppress backward scattering. This can be achieved using high index dielectric material by employing Kerker condition [11]. This condition results from interference between electric and magnetic dipole radiation with opposite phase at backward direction while at forward direction, these radiation are in the same phase. **Figure 6** shows radiation polar plot of single silicon nanosphere with radius of 80 nm at 694 nm incident wavelength. This system is embedded in background medium with refractive index $n_b = 1$ and calculation of forward-backward scattering intensity ratio is performed at far field zone $r \approx 2$ μm .

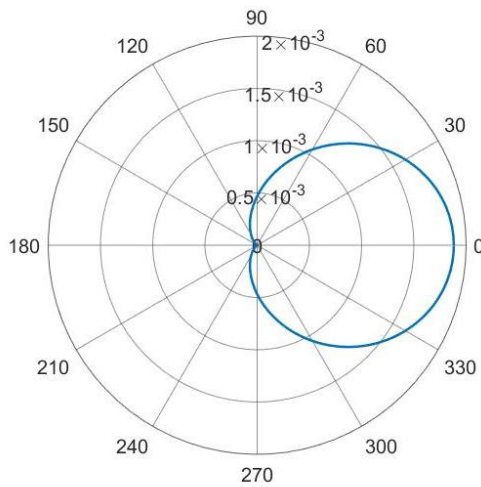


Figure 6. Radiation polar plot (in xz plane) for single silicon nanosphere with radius of 80 nm at 694 nm incident wavelength. This configuration yields Kerker condition which produced suppression of backward scattering.

From **Figure 6**, we can see that this configuration yields zero backward scattering. By choosing appropriate values of radius and incident wavelength, Kerker condition can be achieved which result in suppression of backward scattering. Comparing this result from **Figure 6** (single nanosphere) with the results from **Figure 5** (multiple nanospheres), we can draw several conclusion. At the same far field observation zone (which is $r \approx 2 \mu\text{m}$ in this case), multiple nanospheres produce higher intensity than the single nanosphere does. The shape of radiation pattern from multiple nanosphere has acute opening angle at forward direction (as can be seen from **Figure 3** and **Figure 5**). On the other hand, single nanosphere yields radiation pattern which has much wider angle opening. We can say that the directivity is higher for multiple nanospheres. From the system itself, we can vary the radius of single nanosphere for controlling scattering output while in multiple nanospheres, more variable can be varied such as radius of each spheres and the distance between spheres. Overall, we can say that system of multiple nanospheres give better results and better control compared to single nanosphere in suppressing backward scattering.

4. Conclusion

In this study, we have demonstrated suppression of backward scattering using nanospheres composed of three silicon nanospheres arranged in chain-like configuration. We found that an ideal directed scattered radiation of this system is not only to have a large forward-backward ratio of the scattered field but also a large forward directed scattered field.

We have showed that suppression of backward scattering can be achieved by varying the gap distance between nanospheres at certain incident wavelength. However, to find the optimum geometrical configuration of the structure considered, we perform an analysis of the Mie multipole modes contribution. There is an optimum value for this gap distance which yields the largest ratio. When the distance is increased further, backward scattering will be enhanced due to higher multipole modes excitation. From comparison with single nanosphere, system of multiple nanospheres provide better results and control in suppressing backward scattering.

Acknowledgement

This work is supported by Program Penelitian, Pengabdian Kepada Masyarakat dan Inovasi (P3MI), Institut Teknologi Bandung (1000F/I1.C01/PL/2019).

References

- [1] R S Savelev, S V Makarov, A E Krasnok, and P A Belov, *Optics and Spectroscopy*, **119**(4), 551-568 (2015).
- [2] A E Krasnok, A E Miroshnichenko, P A Belov, and Y S Kivshar, *JETP Letters*, **94**(8), 593-598 (2011).
- [3] P Albella, T Shibanuma, and S A Maier, *Scientific Reports* **5**, 18322 (2015).
- [4] B S Luk'yanchuk, N V Voshchinnikov, R Paniagua-Domínguez, and A I Kuznetsov, *ACS Photonics*, **2**(7), 993-999 (2015).
- [5] Y Zhang, M Nieto-Vesperinas, and J J Sáenz, *Journal of Optics*, **17**(10), 105612 (2015).
- [6] Y L Xu, *Applied Optics* **34**(21), 4573-4588 (1995).
- [7] C. F. Bohren and D. R. Huffman, *Absorption and scattering of light by small particles*, John Wiley & Sons (2008).
- [8] S Mühlig, C Menzel, C Rockstuhl, and F Lederer, *Metamaterials*, **5**(2-3), 64-73 (2011).
- [9] I Staude and J Schilling, *Nature Photonics*, **11**(5), 274 (2017).
- [10] D E Aspnes and A A Studna, *Physical Review B*, **27**(2), 985 (1983).
- [11] M Kerker, D S Wang, and C L Giles, *JOSA*, **73**(6) 765-767 (1983).